Giant acoustoelectric current in suspended quantum point contacts

Dustin J. Kreft,[1] Lev G. Mourokh,[3] Hyuncheol Shin,[1] Max Bichler,[4] Werner Wegscheider,[5] and Robert H. Blick[1,2,6]

[1]*Department of Electrical and Computer Engineering, University of Wisconsin—Madison, Madison, Wisconsin 53706, USA*

[2]*Department of Physics, University of Wisconsin—Madison, Madison, Wisconsin 53706, USA*

[3]*Department of Physics, Queens College of the City University of New York, Flushing, New York 11367, USA*

[4]*Walter-Schottky-Institute, Technical University Munich, Am Coulombwall 4, DE-85748 Garching, Germany*

[5]*Laboratory for Solid State Physics, HPF E 7, ETH Zürich, Schafmattstrasse 16, 8093 Zürich, Switzerland*

[6]*Institute for Nanostructure and Solid State Physics and Center for Hybrid Nanostructures, Hamburg University, Jungiusstrasse 11c, 20355 Hamburg, Germany*

(Received 6 June 2012; revised manuscript received 20 November 2016; published 23 December 2016)

We present results on the acoustoelectric current driven through a quantum point contact (QPC) placed on a suspended nanobridge, which is subject to surface acoustic waves (SAWs). The magnitude of this current is much larger than that of a two-dimensional gas, and the system has enhanced sensitivity to perturbations. In particular, the current oscillations as a function of magnetic field exhibit additional features associated with the spin splitting. Furthermore, the negative voltage applied to the QPC gates induces the oscillations revealing the subband structure not seen in transport measurements at the elevated temperatures of our experiment. Near the pinch off conditions, the acoustoelectric current becomes negative which we attribute to the enhanced backscattering caused by the SAW-phonons' absorption and emission.

DOI: 10.1103/PhysRevB.94.235305

Surface acoustic waves (SAWs) are traditionally employed to investigate low-dimensional electron systems [1–4]. This is mainly due to the fact that acoustic excitations of electron systems deliver complement information as compared to conventional transport measurements. In addition, SAWs are found in existing technological applications, such as in radiofrequency identification (RFID) tags and delay lines [5], as well as in proposals for novel electronic devices [6–8]. Combining SAWs and low-dimensional electron gases naturally allows the study of one-dimensional (1D) systems, so-called quantum point contacts (QPCs).

The ability to create a quantized current, which is immune to impurities and shows stability over changes in source-drain biases and temperature [9], makes high frequency SAWs ideal candidates for quantized current sources in metrology. Many studies have investigated the behavior of SAWs under various conditions, including their response to a magnetic field [10,11] as well as the formation of acoustic shock waves in suspended structures [12]. The most noted application of SAWs with two-dimensional electron gases (2DEGs) is to study electronic transport properties. Since the SAWs produce a clean and constant current, they have been shown to be used to populate and depopulate double quantum dot (DQD) systems [1] and can also be applied for trapping electrons [6] or transferring them [7,8] for the purpose of quantum computing. In other experiments, it has been demonstrated, through the use of QPCs, that the current produced from a SAW can be pinched off through a narrow channel creating a quantized current where the steplike behavior of single-electron transport is easily observed [2,3,9].

In this paper, we present our findings of a system utilizing SAWs across a suspended bridge interacting with a QPC. In pinching off the current produced by the SAWs, we have observed oscillations in the acoustoelectric current which, in turn, changes sign once the applied voltage to the QPC becomes more negative. We get both positive and negative oscillations prior to complete QPC pinch off. The positions of the oscillation peaks correspond to the 1D plateaus seen at standard low-temperature transport measurements [9,13]. At the elevated temperatures of our experiment, the contributions of different subbands are not distinguishable anymore, resulting in the washing out of the conductance steps. However, the subband structure still can manifest itself in the form of the oscillations of the acoustoelectric current. The origin of the current negativity can be better understood in terms of enhanced backscattering [14,15] caused by the strong electron-phonon coupling in suspended systems.

The device under test was fabricated on a $GaAs/Al_{1-x}Ga_xAs$ heterostructure which contains a 2DEG 40 nm below the surface and a 400 nm thick sacrificial layer that lies 90 nm below the surface. Optical lithography was used to carry out the following steps. Firstly, the 2DEG is defined and wet etched. Secondly, four Ohmic contacts are defined and annealed on top of the 2DEG. Thirdly, metallic gates are defined which lead to the QPCs and interdigitated transducer (IDT) fingers. Fourthly, through electron-beam lithography the following steps are carried out: the QPC pairs and the IDT fingers are defined. Fifthly, the acoustic waveguide is defined and etched; and finally, the sacrificial layer is wet etched, leaving a suspended region in the center, see Fig. 1.

The IDTs were fabricated to operate at various frequencies, 840 MHz to ~1.5 GHz, which was chosen based upon $v_s = \lambda f$; where $v_s = 2817\,\mathrm{m/s}$ is the sound velocity of GaAs [16], λ is the wavelength of the SAW (also the pitch of the IDT fingers), and f is the frequency of operation. The spacing between the left and right QPC pairs is about 900 nm. Wavelengths of 2 and 4 μm were used to produce an integer number of waves between the two IDTs, each IDT being 232 μm from the center QPC pair. The acoustic waveguide shown in Fig. 1(a) as an etched trench is as an exponential waveguide [17] positioned at the left and right entrances (mouth). The center straight region where the QPCs reside is a straight pipe, or rectangular, waveguide geometry. The exponential portion of the geometry, which acts as a high

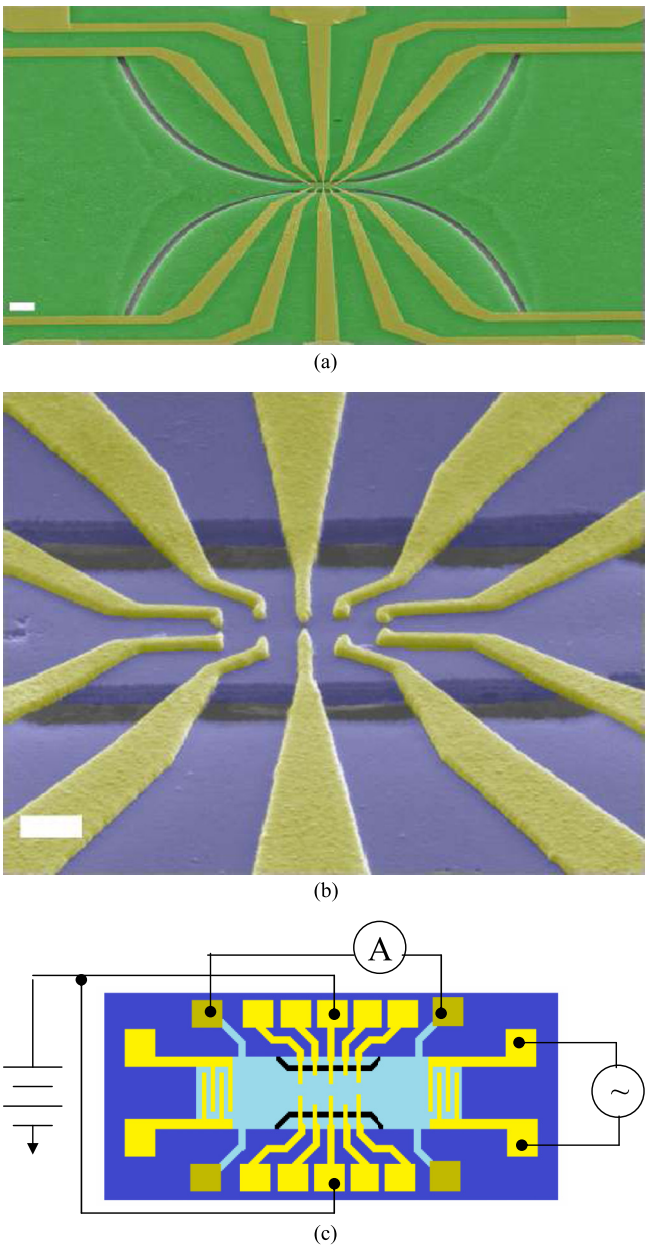

FIG. 1. Scanning electron micrograph (SEM) images of the device. (a) Full view of the etched acoustic waveguide, dark regions indicate the suspended membrane. Scale bar is 2 μm. (b) Close up image of center region, yellow indicates the Ti/Au electrodes which make up the QPC pairs. Scale bar is 300 nm. (c) Schematic diagram of the device and measurement setup, not drawn to scale.

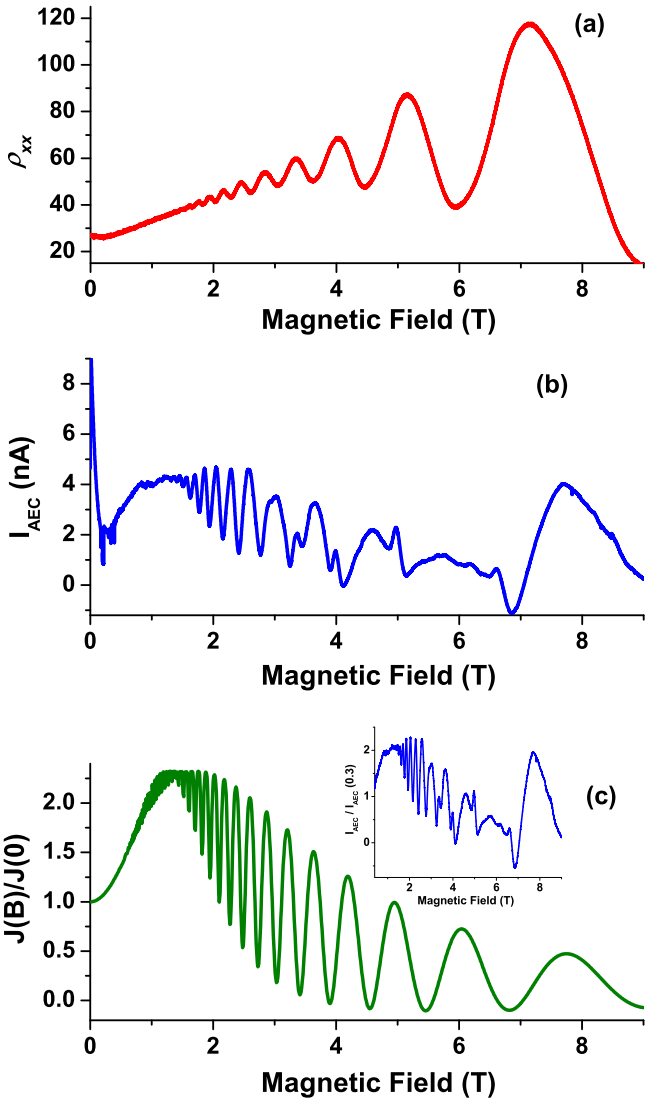

FIG. 2. Hall measurement data (taken with floating gates): (a) Standard Hall measurement as taken with a four-point probe and standard lock-in techniques using a source-drain bias. (b) The acoustoelectric current I_{AEC} was produced using a SAW with no dc bias applied. (c) Theoretical curve for the acoustoelectric current.

pass filter, was fabricated with a cutoff frequency of 75 MHz, which is well below our operational frequencies of $\geqslant$840 MHz. This setup reduces the reactance of the system and causes the two geometries of the waveguide to become impedance matched. This serves two purposes: (1) to couple the SAW power efficiently into the center suspended region of the device where the QPCs are located, and (2) to prevent SAWs from traveling across the outer regions of the suspended bridge where undesired acoustoelectric currents may flow due to SAW reflections. The IDTs have a 50 μm aperture while the opening of the acoustic waveguide extends beyond that to 70 μm. The suspended nanobridge allows a stronger SAW induced phonon coupling to the 2DEG electrons since the phonons cannot dissipate into the bulk material.

To characterize the material, we performed Hall measurements by means of two methods: for the first one, we used a standard lock-in technique with a four-point measurement, see Fig. 2(a). The traditional oscillations are easily visible, as was expected. For the second approach, Fig. 2(b), we used a SAW to generate the current through the device while the acoustoelectric current was measured at two Ohmic contacts using an Ithaco current amplifier. The radio frequency (RF) power applied at the IDT electrodes was -12 dBm and had an operating frequency of 1.488 GHz. The 2DEG has an electron carrier density of $n_e = 4.2\times10^{15}$ m^{-2} and an electron mobility of $\mu_e = 2.57\times10^5$ cm^2/Vs. All measurements were carried out at a base temperature of 4.2 K.

Figure 2(b) shows the acoustoelectric current response of the SAW in the presence of a magnetic field. It can be seen that the oscillations measured in response to the SAW nearly match those of the dc bias of the traditional Hall measurement. The mismatch between the two arises from the difference between two- and four-point measurements, as the contact lead resistance is sampled in the two-point case. Another feature that is evident is the splitting of the peak in the acoustoelectric current trace of Fig. 2(b) between 3 to 4 T. This does not occur in the Hall measurement, and we attribute it to a spin splitting at elevated magnetic fields. At these values, the SAW attenuation, given by [18]

$$\Gamma = k\frac{K_{\text{eff}}^2}{2}\frac{\frac{\sigma_0}{\sigma_m}}{1+\left(\frac{\sigma_0}{\sigma_m}\right)^2}, \tag{1}$$

is maximal which results in a reduced SAW amplitude. Here, k is the wave number, K_{eff} is the electromechanical coupling coefficient for GaAs, $\sigma_0 = e^2 n_e \tau/m^*$ is the Drude conductivity, and $\sigma_m = v_s(\varepsilon_0 + \varepsilon_{\text{GaAs}})$ is a constant of the material. Both σ parameters are taken at zero magnetic field in Eq. (1). The center of the SAW current split is where a minimum occurs in the 2DEG conductivity [10,11].

The acoustoelectric current is proportional to the attenuation, Eq. (1) [18]. Correspondingly, the current at nonzero magnetic field normalized to its value at zero field has the form

$$\frac{J(B)}{J(0)} = \frac{\frac{\sigma(B)}{1+\left[\frac{\sigma(B)}{\sigma_m}\right]^2}}{\frac{\sigma_0}{1+\left(\frac{\sigma_0}{\sigma_m}\right)^2}}, \tag{2}$$

where the conductivity at nonzero field is given by [19]

$$\sigma(B) = \frac{\sigma_0}{1+\omega_c^2\tau^2}\left(1 - \frac{2\omega_c^2\tau^2}{1+\omega_c^2\tau^2}\frac{2\pi^2 k_B T}{\hbar\omega_c}\text{csch}\left\{\frac{2\pi^2 k_B T_e}{\hbar\omega_c}\right\} \times \cos\left\{\frac{2\pi^2 E_F}{\hbar\omega_c}\right\}\exp\left\{-\frac{\pi}{\omega_c\tau}\right\}\right), \tag{3}$$

with ω_c being the cyclotron frequency. The normalized acoustoelectric current, Eq. (2), is shown in Fig. 2(c). We present the normalized current of Fig. 2(b) in the inset, and it is evident that the main experimental features, such as the oscillations with respect to magnetic field, increase and subsequent decrease in magnitude, and the initial increase of the current are well reproduced. We normalize the current to its value at $B = 0.3$ T to eliminate the behavior at very low field, the origin of which is still unclear. Equation (3) is valid for our range of parameters because the product $\omega_c\tau$ is less than one for $\tau = 5\times10^{-14}$ s and the magnetic field of our experiment [18]. The electron spin is not included in Eq. (3), so the peak splitting at large field is not seen at the theoretical curve.

The next step is to determine the behavior of the SAW interactions with the QPCs of the device. First, we characterize the behavior of the QPCs; in this paper, we focus on only the center QPC pair (see Fig. 1). We applied a dc source-drain bias V_{SD} to two of the Ohmic contacts while sweeping the gate voltage of the center QPC at zero magnetic field, see Fig. 3. It should be noted that usual conductance steps are already washed out at the elevated temperatures of our experiment [20], but they would appear at the gate voltages

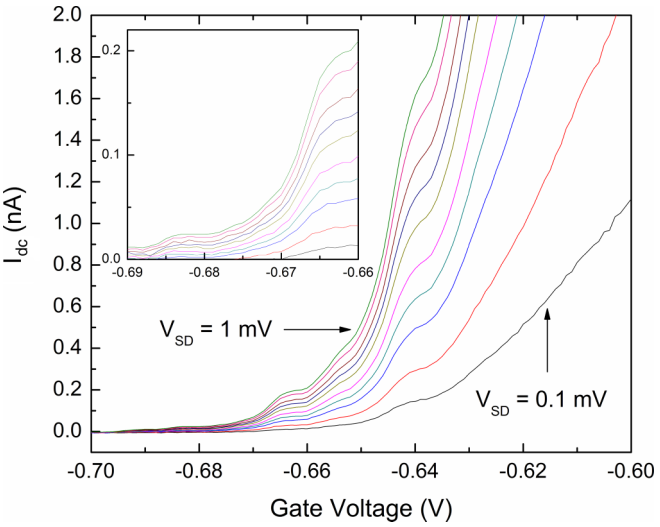

FIG. 3. Applied dc source-drain bias pinch off with V_{SD} ranging from 0.1 to 1 mV in 0.1 mV increments. Inset shows a magnified view of the current with the gate voltage ranging from −0.69 to −0.66 V. Measurements are performed at zero magnetic field.

in the region of −0.8 and −0.7 V. The plateaulike features which can be seen at smaller negative voltages correspond to the transition from 1D to 2D transport [21]. The measured current is rather small in comparison to usual values for 2DEG at these temperatures. We attribute this phenomenon to enhanced incoherent electron-phonon interaction for our suspended nanobridge structure. We then proceed to generate the dc current through the use of SAWs. An applied RF power of −10 dBm at a frequency of 840 MHz is applied to the right IDT of the sample, see Fig. 1(c); the results can be viewed in Fig. 4(a). It should be emphasized that the magnitude of the acoustoelectric current is up to 15 nA, which exceeds that of the usual 2DEG with SAW, without the suspended nanobridge (up to 1 nA [9]). Moreover, it exceeds the source-drain current without SAW in suspended nanobridge by one or two orders of magnitude in the regime of small gate voltages, see Fig. 3. We expected to see a steplike behavior in the acoustoelectric current pinch off with quantized steps, similar to what is reported of a standard source-drain bias pinch off [2–3]; however, we observe oscillatory behavior in the measured current. Similar results were obtained in Refs. [9,13,21,22], and several theoretical models were subsequently proposed [14,15].

These oscillations were attributed to the subband formation in the QPC. When the 1D subband is about to be depopulated, the electron velocity becomes very small, comparable to the sound velocity. In this case, the interaction of electrons to the SAW is maximal, resulting in a maximum of the acoustoelectric current. It should be noted that, at the temperature of 4.2 K, the conductance steps are already washed out because, at given gate voltage, there are contributions from several subbands, and they cannot be separated in standard transport measurements. However, the 1D subbands still exist, and due to the strong coupling of electrons to the SAW within the suspended nanobridge region, their manifestations are observed in the acoustoelectric current.

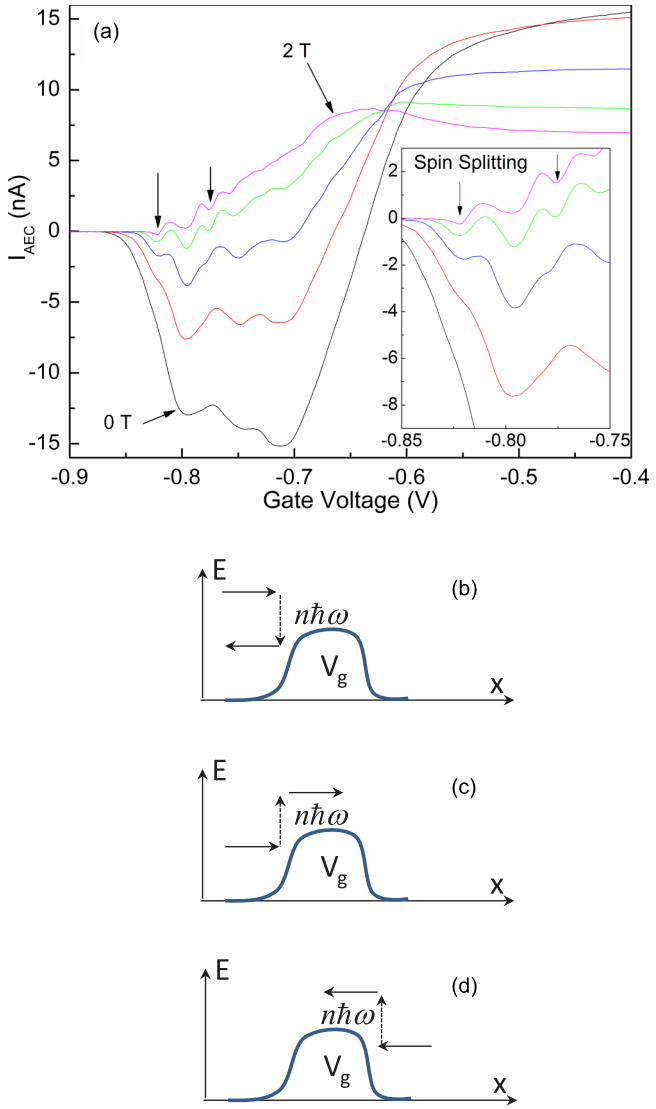

FIG. 4. (a) Acoustoelectric current at magnetic fields of 0, 0.5, 1.0, 1.5, and 2.0 T. Applied RF power of −10 dBm and a frequency of 840 MHz. Inset shows a subset of the data detailing the spin splitting that starts to become visible at 1 T. (b) Inelastic scattering of an electron emitting n phonons of $\hbar\omega$, causing backscattering from the QPC gate potential V_g. (c) Inelastic scattering of an electron absorbing n phonons of $\hbar\omega$, allowing it to scatter forward across the QPC gate potential V_g. (d) Electron absorbing n phonons and scattering to the left.

With a significant magnetic field applied, the 1D subbands become spin split. The manifestations of this effect are shown in Fig. 4(a) as the shoulder formation at 1 T with additional minima at 1.5 and 2 T. These features support our conclusions of oscillations being consequences of the QPC subband structure. The wide broadening of the oscillations is due to the higher temperature at which our measurements were taken when compared to narrow oscillations of measurements at lower temperatures [12,13]. It should be emphasized that the spin splitting can be seen at quite low magnetic field [lower than that of Fig. 2(b)] due to the enhanced sensitivity to external perturbations which is exhibited by the QPC near the pinch off conditions.

The current starts to become negative around −0.65 V at 0 T. The source-drain bias current reaches complete pinch off just below −0.7 V. This behavior seems to be more noticeable when the channel length of the QPC is comparable to the SAW wavelength but is still valid for larger wavelengths. In our sample, the defined channel length is ∼80 nm, compared to other experiments where the channel length is from several hundred nanometers to the order of microns. This narrow channel length opens the possibility of backscattering [14,15].

As shown in Fig. 4(a), the acoustically driven current starts off with a positive amplitude of 12 to 16 nA but becomes negative due to phonon scattering as the gate voltage decreases. This change in gate voltage changes the effective length of the QPC channel as well as the transmission probabilities for electrons to scatter forward or backward. When the gate voltage is low or zero, the electrons pass through the channel without any scattering since the potential is low. As the gate potential further decreases, the barrier becomes larger, causing a small amount of backscattering, see Fig. 4(b), which reduces the current. It should be noted that electrons moving against the source-drain bias ($V_{SD} = 0.05$ mV in our experiment) and having energy smaller than the top of the QPC barrier can still proceed after the absorption of phonons, see Fig. 4(d). Once the gate voltage is decreased to about −0.65 V, the scattering events cause equal transmission in both directions, thus a zero net current. Below this level, −0.65 V, the potential barrier is increased enough to cause the electrons to backscatter; hence, inducing a negative net current until complete pinch off is achieved. As the finite source-drain potential is applied, we are able to differentiate between forward and backward current. Hence, it is accurate to state this is phonon induced since these features do not appear when SAWs are absent, see Fig. 3. Figures 4(b)–4(d) [14,15] show that the phonon background interacts with the electrons present near the QPC induced potential. The energy of a single phonon $\hbar\omega$ is much smaller than the conduction window $\delta E = eV_{SD}$, but extremely strong electron-phonon coupling in suspended nanobridge enhances the probability of emission/absorption of n phonons which makes the effect more pronounced than that of the structures made with the usual 2DEG.

In summary, we were able to achieve an extremely strong acoustoelectric response of a suspended QPC, even at an elevated temperature of 4.2 K. The oscillatory features from pinch off that we have observed fit well with existing theory, proving the advantage of a suspended system which allows an order of magnitude larger electron-phonon coupling. It was also seen that the 1D subband structure and its spin splitting become detectable at these higher temperatures. From our results, we were able to produce a theoretical model that accurately describes the acoustoelectrically generated current through a 2DEG in the presence of a perpendicular magnetic field. Due to the inherently strong SAW interactions with suspended 2DEGs, this system has proven valid for high temperature measurements for future applications.

We would like to thank the National Science Foundation (NSF) for support under Grant No. ECCS-0708759. RHB would like to thank the Air Force Office for Scientific Research (AFOSR) for support through a Multi-University-Research-Initiative'08 Grant (No. FA9550-08-1-0337).

[1] M. Kataoka, R. J. Schneble, A. L. Thorn, C. H. W. Barnes, C. J. B. Ford, D. Anderson, G. A. C. Jones, I. Farrer, D. A. Ritchie, and M. Pepper, Phys. Rev. Lett. **98**, 046801 (2007).
[2] V. I. Talyanskii, J. M. Shilton, M. Pepper, C. G. Smith, C. J. B. Ford, E. H. Linfield, D. A. Ritchie, and G. A. C. Jones, Phys. Rev. B **56**, 15180 (1997).
[3] L. Song, S. W. Chen, J. H. He, C. Y. Zhang, C. Lu, and J. Gao, Solid State Commun. **150**, 292 (2010).
[4] C. C. W. Ruppel and T. A. Fjeldy, *Advances in Surface Acoustic Wave Technology, Systems and Applications* (World Scientific, Singapore, 2001), Vol. 2.
[5] C. Campbell, *Surface Acoustic Wace Devices for Mobile and Wireless Communications* (Academic Press, San Diego, CA, 1998).
[6] C. H. W. Barnes, J. M. Shilton, and A. M. Robinson, Phys. Rev. B **62**, 8410 (2000).
[7] S. Hermelin, S. Takada, M. Yamamoto, S. Tarucha, A. D. Wieck, L. Saminadayar, C. Bäuerle, and T. Meunier, Nature **477**, 435 (2011).
[8] R. P. G. McNeil, M. Kataoka, C. J. B. Ford, C. H. W. Barnes, D. Anderson, G. A. C. Jones, I. Farrer, and D. A. Ritchie, Nature **477**, 439 (2011).
[9] J. M. Shilton, V. I. Talyanskii, M. Pepper, D. A. Ritchie, J. E. F. Frost, C. J. B. Ford, C. G. Dmith, and G. A. C. Jones, J. Phys.: Condens. Matter. **8**, L531 (1996).
[10] A. Wixforth, J. Scriba, M. Wassermeier, J. P. Kotthaus, G. Weimann, and W. Schlapp, Phys. Rev. B **40**, 7874 (1989).
[11] D. J. Kreft and R. H. Blick, in *Surface Acoustic Waves and Nano-Electromechanical Systems, Acoustic Waves—From Microdevices to Helioseismology*, edited by M. G. Beghi (InTech, Rijeka, Croatia, 2011).
[12] F.W. Beil, A. Wixforth, W. Wegscheider, D. Schuh, M. Bichler, and R. H. Blick, Phys. Rev. Lett. **100**, 026801 (2008).
[13] J. M. Shilton, D. R. Mace, V. I. Talyanskii, Y. Galperin, M. Y. Simmons, M. Pepper, and D. A. Ritchie, J. Phys.: Condens. Matter. **8**, L337 (1996).
[14] F. A. Maaø and Y. Galperin, Phys. Rev. B **56**, 4028 (1997).
[15] H. Totland, Ø. L. Bø, and Y. M. Galperin, Phys. Rev. B **56**, 15299 (1997).
[16] J. Sapriel, J. C. Michel, J. C. Tolédano, R. Vacher, J. Kervarec, and A. Regreny, Phys. Rev. B **28**, 2007 (1983).
[17] V. Salmon, JASA **17**, 212 (1946).
[18] Y. Ilisavskii, A. Goltsev, K. Dyakonov, V. Popov, E. Yakhkind, V. P. Dyakonov, P. Gierlowski, A. Klimov, S. J. Lewandowski, and H. Szymczak, Phys. Rev. Lett. **87**, 146602 (2001).
[19] T. Ando, A. B. Fowler, and F. Stern, Rev. Mod. Phys. **54**, 437 (1982).
[20] B. J. van Wees, L. P. Kouwenhoven, E. M. M. Willems, C. J. P. M. Harmans, J. E. Mooij, H. van Houten, C. W. J. Beenakker, J. G. Williamson, and C. T. Foxon, Phys. Rev. B **43**, 12431 (1991).
[21] K. J. Thomas, J. T. Nicholls, M. Y. Simmons, M. Pepper, D. R. Mace, and D. A. Ritchie, Phys. Rev. Lett. **77**, 135 (1996).
[22] F. J. Ahlers, N. E. Fletcher, J. Ebbecke, and T. J. B. M. Janssen, Current Appl. Phys. **4**, 529 (2004).